

Original article

DOI: <https://doi.org/10.18721/JPM.15305>

SIMULATION OF AN UNSTEADY FLOW AND MIXING OF FINE GAS SUSPENSION IN A CLOSED VOLUME BY THE HYBRID METHOD OF LARGE PARTICLES

E. N. Shirokova✉

Military Space Academy named after A. F. Mozhaysky, St. Petersburg, Russia

✉ shirokhelen-78@mail.ru

Abstract. Hydrodynamic effects of convective transport and mixing of dispersed reagents determine the efficiency of chemical reactions in some cases. The paper sets and numerically solves the problem of a pulsed outflow and mixing of gas suspension in a volume limited by walls. The initial dispersed-phase concentration at which an anomalous subsonic regime (with the shock-wave structure formation) is replaced by supersonic one (as to the velocity of the carrier gas phase) has been found. It was established that phenomena of instability development and eddying dominate for a long-time interval. The resolution of the hybrid large-particles method was demonstrated for this class of problems.

Keywords: gas suspension, shock-wave structure, convective transport, mixing, hybrid large-particle method

Citation: Shirokova E. N., Simulation of an unsteady flow and mixing of fine gas suspension in a closed volume by the hybrid method of large particles, St. Petersburg Polytechnical State University Journal. Physics and Mathematics. 15 (3) (2022) 61–70. DOI: <https://doi.org/10.18721/JPM.15305>

This is an open access article under the CC BY-NC 4.0 license (<https://creativecommons.org/licenses/by-nc/4.0/>)

Научная статья

УДК 532/529

DOI: <https://doi.org/10.18721/JPM.15305>

МОДЕЛИРОВАНИЕ НЕСТАЦИОНАРНОГО ТЕЧЕНИЯ И ПЕРЕМЕШИВАНИЯ МЕЛКОДИСПЕРСНОЙ ГАЗОВЗВЕСИ В ЗАМКНУТОМ ОБЪЕМЕ ГИБРИДНЫМ МЕТОДОМ КРУПНЫХ ЧАСТИЦ

Е. Н. Широкова✉

Военно-космическая академия имени А. Ф. Можайского, Санкт-Петербург, Россия

✉ shirokhelen-78@mail.ru

Аннотация. Гидродинамические эффекты конвективного переноса и перемешивания диспергированных реагентов в ряде случаев определяют результативность протекания химических реакций. В работе поставлена и численно решена задача импульсного истечения и перемешивания газозвеси в объеме, ограниченном стенками. Определена начальная концентрация дисперсной фазы, при которой происходит смена аномального дозвукового режима течения (с образованием ударно-волновой структуры) сверхзвуковым режимом (по скорости несущей газовой фазы). Установлено, что при длительном временном интервале доминируют явления развития неустойчивости и образования вихрей. Продемонстрирована разрешающая способность гибридного метода крупных частиц для данного класса задач.

Ключевые слова: газозвесь, ударно-волновая структура, конвективный перенос, перемешивание, гибридный метод крупных частиц

Ссылка для цитирования: Широкова Е. Н. Моделирование нестационарного течения и перемешивания мелкодисперсной газозвеси в замкнутом объеме гибридным методом крупных частиц // Научно-технические ведомости СПбГПУ. Физико-математические науки. 2022. Т. 15. № 3. С. 61–70. DOI: <https://doi.org/10.18721/JPM.15305>

Статья открытого доступа, распространяемая по лицензии CC BY-NC 4.0 (<https://creativecommons.org/licenses/by-nc/4.0/>)

Introduction

Chemical technologies are based on complex interrelated hydromechanical phenomena (fluidization, precipitation, mixing), chemical processes (synthesis, catalysis, oxidation) and those related to heat and mass transfer (evaporation, condensation, crystallization) [1–4]. Methods of mathematical modeling are now widely used in the chemical industry. The effects of wave and convective transfer as well as mixing of dispersed chemicals play a major role in different technological processes.

Numerical methods for studying hydrodynamic phenomena are associated with mesh-based reconstruction of shock-wave processes, which are satisfactorily resolved within the framework of Euler equations. Simulation of various types of instabilities, mixing and turbulence generally requires more complex approaches, which are traditionally divided into methods of direct numerical simulation (DNS), large eddy simulation (LES) and Reynolds averaged Navier–Stokes equations (RANS), or their hybrid combinations [5, 6].

The conservation laws generally include the convective and diffusive (viscous) terms of equations in differential or integral form and the right-hand sides depending on the solution (sources). The resolution of a numerical method is largely determined by the level of numerical dissipation provided for approximating the convective terms of equations. For example, the accuracy of second and third-order convective schemes CFX and FLUENT packages was analyzed in [7]. Modern methods for mathematical modeling of hydrodynamic instabilities and turbulent mixing were reviewed in [8], focusing on approximation of convective flows in various numerical schemes.

The performance and dissipative properties of numerical methods approximating the flux terms are typically estimated by solving test problems in an inviscid formulation, for example, simulating the Rayleigh–Taylor [9], Kelvin–Helmholtz [10] and Richtmyer–Meshkov instabilities [11]. The discontinuities are smoothed, and the eddies are reconstructed to some degree, depending on the dissipative properties of the numerical schemes.

Simulation of two-phase flows encounters a number of additional fundamental problems [12]. One of them is rigidity of the problems including fast and slow components of the solution. This problem was apparently first formulated and solved for dispersed-gas systems in [13]. The problems of free and impact two-phase jet flows and cylindrical expansion of gas suspensions were numerically and experimentally considered in [14–16].

Our study considers a new formulation of the problem on the gas dynamics of wave and convective transfer and mixing of ideal carrier gas and suspended solid particles in pulsed outflow into a closed volume.

Constitutive equations

We write the conservation laws for dispersed gas in the formulation for interpenetrating continua [17]:

$$\begin{aligned} \frac{\partial \rho_i}{\partial t} + \nabla \cdot (\rho_i \mathbf{v}_i) &= 0, \quad \frac{\partial}{\partial t} (\rho_1 \mathbf{v}_1) + \nabla \cdot (\rho_1 \mathbf{v}_1 \mathbf{v}_1) + \alpha_1 \nabla p = -\mathbf{F}_\mu, \\ \frac{\partial}{\partial t} (\rho_2 \mathbf{v}_2) + \nabla \cdot (\rho_2 \mathbf{v}_2 \mathbf{v}_2) + \alpha_2 \nabla p &= \mathbf{F}_\mu, \quad \frac{\partial}{\partial t} (\rho_2 e_2) + \nabla \cdot (\rho_2 e_2 \mathbf{v}_2) = Q, \\ \frac{\partial}{\partial t} (\rho_1 E_1 + \rho_2 E_2) + \nabla \cdot (\rho_1 E_1 \mathbf{v}_1 + \rho_2 E_2 \mathbf{v}_2) + \nabla \cdot [p(\alpha_1 \mathbf{v}_1 + \alpha_2 \mathbf{v}_2)] &= 0, \\ \rho_i &= \rho_i^\circ \alpha_i, \quad (i = 1, 2), \quad \alpha_1 + \alpha_2 = 1, \quad \rho = \rho_1 + \rho_2, \quad E_i = e_i + \mathbf{v}_i^2 / 2, \end{aligned} \quad (1)$$



where α_i , ρ_i , \mathbf{v}_i , E_i , e_i , p are the volume fraction, the reduced density (kg/m³), the velocity vector (m/s), the total and internal energy (J/kg) of the i th component of the continuum ($i = 1$ for gas or $i = 2$ for dispersed phase), the gas pressure (Pa), respectively; \mathbf{F}_μ , Q are the frictional force (N/m³) and the heat transfer rate (W/m³) between gas and particles; t , s , is the time; the superscript \circ indicates the true densities of gas and particle material.

System of equations (1) is closed by the equation of state for calorically perfect ideal gas and incompressible solid particles:

$$p = (\gamma_1 - 1)\rho_1^\circ e_1, \quad e_1 = c_v T_1, \quad e_2 = c_2 T_2, \quad \{\gamma_1, c_v, c_2, \rho_2^\circ\} \equiv \text{const},$$

where T_1 , T_2 , K, are the temperatures of the carrier phase and particles; γ_1 , c_v , J/(kg·K), are the adiabatic index and specific heat capacity of the gas at constant volume; c_2 , J/(kg·K), is the specific heat capacity of the particles.

Interfacial friction and heat transfer \mathbf{F}_μ , Q_T are determined from empirical dependences [18]:

$$\mathbf{F}_\mu = (3/8)(\alpha_2 / r) C_\mu (\text{Re}_{12}) \rho_1 (\mathbf{v}_1 - \mathbf{v}_2) |\mathbf{v}_1 - \mathbf{v}_2|,$$

$$C_\mu = \begin{cases} C_\mu^{(1)} = \frac{24}{\text{Re}_{12}} + \frac{4.4}{\text{Re}_{12}^{1/2}} + 0.42, & \alpha_2 \leq 0.08, \\ C_\mu^{(2)} = \frac{4}{3\alpha_1} \left(1.75 + \frac{150\alpha_2}{\alpha_1 \text{Re}_{12}} \right), & \alpha_2 \geq 0.45, \\ \frac{(\alpha_2 - 0.08)C_\mu^{(2)} + (0.45 - \alpha_2)C_\mu^{(1)}}{0.37}, & 0.08 < \alpha_2 < 0.45, \end{cases}$$

$$Q_T = (3/2)(\alpha_2 / r^2) \lambda_1 \text{Nu}_1 (T_1 - T_2),$$

$$\text{Nu}_1 = \begin{cases} 2 + 0.106 \text{Re}_{12} \text{Pr}_1^{1/3} & (\text{Re}_{12} \leq 200), \\ 2.274 + 0.6 \text{Re}_{12}^{0.67} \text{Pr}_1^{1/3} & (\text{Re}_{12} > 200), \end{cases}$$

$$\text{Re}_{12} = 2r\rho_1^\circ |\mathbf{v}_1 - \mathbf{v}_2| / \mu_1, \quad \text{Pr}_1 = c_v \gamma_1 \mu_1 / \lambda_1,$$

where Re_{12} , Nu_1 , Pr_1 are the Reynolds, Nusselt and Prandtl numbers, respectively; C_μ , μ_1 , r , are the coefficient of interfacial friction, dynamic viscosity (Pa·s) and particle radius (m).

Problem statement and computational procedure

Consider the axisymmetric problem on pulsed outflow of gas suspension from cylindrical channel 1 with the length $L = 0.1$ m and the radius $R = 0.01$ m into closed volume 2 (Fig. 1). At the initial moment of time, The channel is filled with a static mixture of high-pressure air ($p^{(1)} = 10^6$ Pa) and solid particles with a diameter of $d = 1$ μm , a density of $\rho_2^\circ = 2500$ kg/m³ at thermodynamic equilibrium of $T^{(1)}_1 = T^{(1)}_2 = 293$ K. The disperse phase occupies a volume fraction of $\alpha^{(1)}_2 = 0.1$. Pure air with the parameters $p^{(2)} = 10^5$ Pa, $T^{(2)}_1 = 293$ K fills closed volume 2 outside the channel. No-slip conditions are imposed at the boundaries (the normal components of the phases are equal to zero).

Numerical simulation was based on a hybrid large-particle method [19] with centered hybrid reconstruction of phase flows in the form given in [20], suitable for solving stiff problems. The calculations are performed in a cylindrical coordinate system on a uniform mesh with the spacing of $h = L/400$ m. The time step was determined by the Courant number $\text{CFL} = 0.4$.

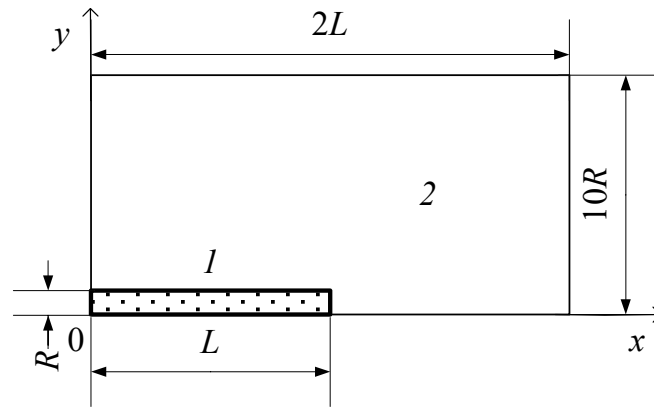


Fig. 1. Computational scheme of the problem (up to the symmetry axis 0x): Channel 1 of length L and radius R ; closed volume 2

Computational results

For convenience, the computational results are given in dimensionless form. Channel length L is selected as the linear scale. The phase pressures and densities are taken relative to the corresponding initial parameters in the channel, $p^{(1)}$ and $\rho^{(1)}$. The phase velocities are normalized by two values: the local speed of sound in the carrier gas $a_1 = (\gamma_1 p / \rho_1)^{1/2}$ or the local effective velocity of the mixture $a_e = [\gamma_e p / (\rho \alpha_1)]^{1/2}$. The effective polytropic index of the two-phase medium in the formula for a_e is found from the expression [19]:

$$\gamma_e = (x_1 c_v + x_2 c_2 + x_1 R_1) / (x_1 c_v + x_2 c_2),$$

where $x_i = \rho_i / \rho$ are the mass fractions of the phases, R_1 , J/(kg·K), is the gas constant.

Time was counted in dimensionless form (Strouhal numbers) $Sh = a_e t / L$. For example, the time instant $Sh = 1$ corresponds to the arrival of an equilibrium rarefaction wave after the initial discontinuity decays to the bottom of the channel.

The initial stage of outflow at $Sh = 0.5$ is shown in Fig. 2, *a* as a distribution of Mach numbers $M = u_2 / a_1$ over a continuous grayscale. The bottom panel of the figure (Fig. 2, *b*) shows numerical schlieren images for the relative density gradient of the dispersed phase $S(\rho_2 / \rho_2^{(1)})$, calculated by the technique described in [21].

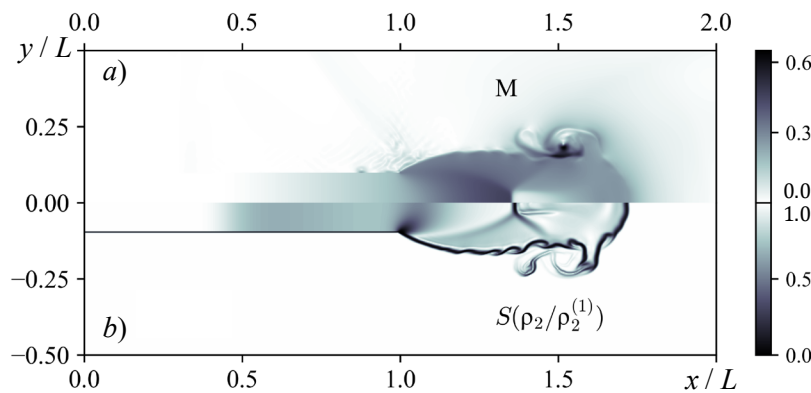


Fig. 2. Distribution of Mach numbers M in a continuous gray scale (*a*); numerical schlieren images $S(\rho_2 / \rho_2^{(1)})$ as functions of the relative density gradient of the dispersed phase (*b*) (both graphs are given for the time instant $Sh = 0.5$)



The rarefaction wave front inside the channel reached the relative coordinate $x/L = 0.5$ at the considered instant $Sh = 0.5$. The first barrel shock with the Mach disk, located in the section $x/L = 1.3$, formed in the outflowing gas suspension. Primary and secondary vortex rings evolved in the head of the jet. A Kelvin–Helmholtz vortex instability develops on the side surface of the jet, visualized on the schlieren image in Fig. 2. As seen from the distribution of the Mach number, the shock-wave structure is anomalously formed in subsonic flow of carrier gas. This phenomenon was previously detected, as well as confirmed numerically and experimentally in a number of works, for example, in [14].

Bow shocks in pure gas typically form in supersonic flow. In view of this, it seems interesting to determine the concentrations of particles for which the flow regime of the gas suspension changes. For this purpose, we carried out a series of computations with above the initial data but changing the initial concentrations of the dispersed phase: $\alpha_2^{(1)} = 0.01; 0.02; 0.10$. Results are given in Fig. 3,*a* as axial distributions of Mach numbers, calculated from the local velocity of the carrier gas. The two-phase medium inside the channel in the region $0.5 < x/L < 1$ is accelerated in a one-dimensional rarefaction wave. Phase velocities in the outlet section of the tube with $x/L = 1$ are subsonic for the given particle concentrations. Their analytical values, calculated by Eqs. (19), are marked by symbols in Fig. 3,*a*.

The gas suspension subsequently accelerates after the nozzle exit to the Mach disk $1 < x/L < 1.3$ as an underexpanded two-dimensional jet. The two-phase medium at initial particle concentrations is accelerated to supersonic speeds of the carrier gas at a certain distance from the exit section. Conversely, the flow of the mixture along the symmetry axis is subsonic everywhere at $\alpha_2^{(1)} > 0.02$.

The reason for the anomaly is that a gas-dispersed medium with sufficiently fine particles acts as a ‘heavy gas’ whose equation of state and effective speed of sound are different from pure gas. Fig. 3,*b* shows the distributions of the Mach number normalized by the local effective speed of sound in a two-phase medium. Notably, the curves $M_e = u_2/a_e$ at the range of the rarefaction wave up to the Mach disk $0.5 < x/L < 1.3$ almost coincide for different particle concentrations in this representation. The flow velocity in the throat section, at $x/L = 1$, is equal to the local speed of sound $M_e = 1$. The gas suspension flow past the nozzle exit accelerates to supersonic velocities in a scale of a_e , up to the bow shock.

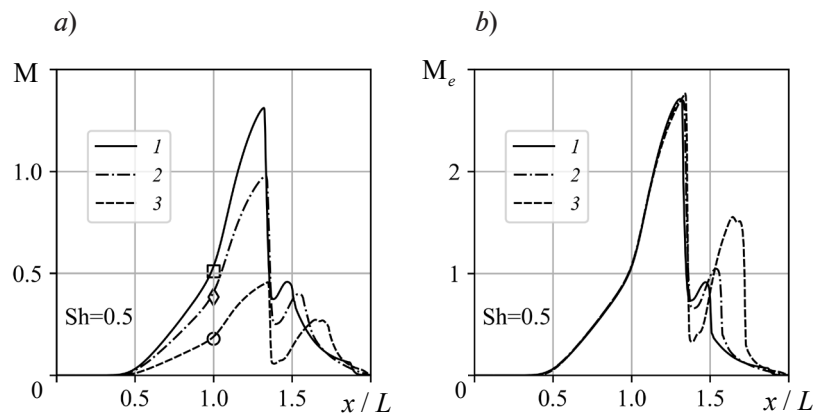


Fig. 3. Axial distributions of Mach numbers at time $Sh = 0.5$, computed from the local speed of sound in the carrier gas phase (*a*) and the local effective velocity of the mixture (*b*), for the initial concentrations of the dispersed phase $\alpha_2^{(1)}$: 0.001 (1); 0.02 (2); 0.10 (3).

The symbols correspond to the analytical values of Mach numbers in the critical section for the given concentrations

Table

Maximum volume fractions of particles at dimensionless times

Sh	1	2	3	4	5	6
α_{\max}	0.093	0.158	0.147	0.090	0.075	0.049

The time evolution of the gas suspension is shown as numerical schlieren images for the relative density gradient of dispersed phase $S(\rho_2/\rho_2^{(1)})$ in Fig. 4. The head of the two-phase jet reaches the wall at dimensionless time $Sh = 0.72$ with $x/L = 2$. After that, its radial expansion begins (Fig. 4,*a*). The lateral structure of two-phase flow along the symmetry axis persists until approximately $Sh \approx 2$. It subsequently decays, with predominantly vortical flow observed (Fig. 4, *c–f*). The closed volume is largely filled by the time $Sh \approx 6$, with gas suspension mixing within it.

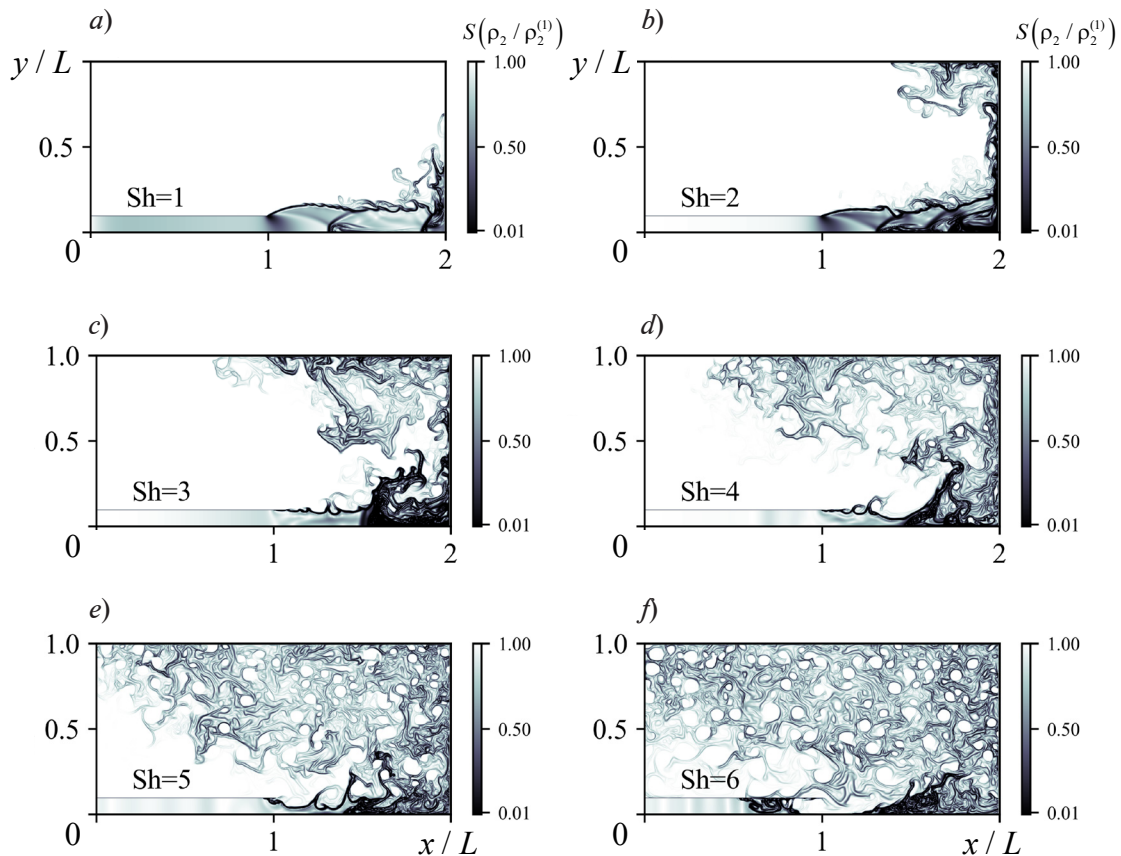


Fig. 4. Numerical schlieren images for relative density gradient of dispersed phase at successive points in time ($Sh = 1–6$)

The volume fraction of particles does not reach the state of dense packaging during the process. The table gives the maximum values for the volume fractions of particles α_{\max} in the entire flow field for successive dimensionless times Sh .

The pressure in the dispersed phase p_d was estimated by a more generalized model of the gas suspension [14]. The quantity p_d was estimated assuming equilibrium for the competing processes of chaotic particle motion generated by the Magnus forces and vortex flow of particles, as well as dissipation of chaotic rotation, translational motion and collisions of dispersed particles. Considering sufficiently fine chemical particles with a diameter of $d = 1 \mu\text{m}$ in the range of relative motion of the mixture components $0 < |\mathbf{v}_1 - \mathbf{v}_2| < 100 \text{ m/s}$, the pressure in the dispersed phase p_d is two orders of magnitude smaller than the gas dynamic pressure p in the carrier phase. The obtained estimate suggests that the collisionless model (1) is well applicable.

Correct simulation of this stage in the process, determining the turbulent characteristics, involves DNS, LES, RANS turbulence models or their combinations. At the same time, the qualitative picture of the flow is reconstructed satisfactorily. In addition, studies of instabilities developing in heterogeneous media established quantitative agreement between the data for the deformation and averaged dynamics of the interfaces obtained experimentally and computationally by various methods, for example, in simulations of the Richtmyer–Meshkov instability [22].



The hybrid large particle method provided high resolution and low dissipation for approximating the convective terms in the conservation laws on a moderately refined mesh for the problem considered.

Conclusion

A hybrid large-particle method was applied within the framework of interpenetrating continua to numerically solve the problem on pulsed outflow of the gas suspension into a volume limited by solid walls. Two characteristic time ranges of the process have been established. The wave effects on the flow of two-phase mixture with a shock-wave structure evolving are predominant at the initial stage. A series of computations yielded an initial concentration of the dispersed phase at which the flow mode is converted from anomalous subsonic to supersonic along the carrier gas phase. Developing instabilities and eddying prevail during the second time range. The capabilities of the hybrid large-particle method have been demonstrated for this class of problems. The method has low numerical viscosity in approximating the convective part of the equations and can serve as a basis for constructing numerical schemes to simulate turbulent flows of gas suspensions. We plan to make this problem the subject of our future studies.

REFERENCES

1. **Huilin L., Gidaspow D., Bouillard J., Wentie L.**, Hydrodynamic simulation of gas-solid flow in a riser using kinetic theory of granular flow, *Chem. Eng. J.* 95 (1–3) (2003) 1– 13.
2. **Zi C., Sun J., Yang Y., et al.**, CFD simulation and hydrodynamics characterization of solids oscillation behavior in a circulating fluidized bed with sweeping bend return, *Chem. Eng. J.* 307 (1 January) (2017) 604– 620.
3. **Gao X., Li T., Rogers W. A., et al.**, Validation and application of a multiphase CFD model for hydrodynamics, temperature field and RTD simulation in a pilot-scale biomass pyrolysis vapor phase upgrading reactor, *Chem. Eng. J.* 388 (15 May) (2020) 124279.
4. **Luge I. A., Bentzon J. R., Klingaa C. G., et al.**, Scale attachment and detachment: The role of hydrodynamics and surface morphology, *Chem. Eng. J.* 430, P. 2 (15 February) (2022) 132583.
5. **Volkov K. N., Emelyanov V. N.**, Modelirovaniye krupnykh vikhrey v raschetakh turbulentnykh techeniy [Large-eddy simulation of turbulent flows], Publishing House of Phys. & Math. Literature, Moscow, 2008 (in Russian).
6. **Garbaruk A. V.**, Sovremennyye podkhody k modelirovaniyu turbulentnosti [Modern approaches to turbulence simulation], Publishing House of Polytechnical Univ., St. Petersburg, 2016 (in Russian).
7. **Isaev S.A., Lysenko D.A.**, Testing of numerical methods, convective schemes, algorithms for approximation of flows, and grid structures by the example of a supersonic flow in a step-shaped channel with the use of the CFX and fluent packages, *J. Eng. Phys. Thermophys.* 82 (2) (2009) 321–326.
8. **Tishkin V. F., Gasilov V. A., Zmitrenko N. V., et al.**, Modern methods of mathematical modeling of the development of hydrodynamic instabilities and turbulent mixing, *Matem. Mod.* 32 (8) (2020) 57–90 (in Russian).
9. **Shi J., Zhang Y.-T., Shu C.-W.**, Resolution of high order WENO schemes for complicated flow structures, *J. Comput. Phys.* 186 (2) (2003) 690–696.
10. **Li J., Shu C.-W., Qiu J.**, Multi-resolution HWENO schemes for hyperbolic conservation laws, *J. Comput. Phys.* 2021. Vol. 446 (1 December) (2021) 110653.
11. **Wang B., Xiang G., Hu X. Y.**, An incremental-stencil WENO reconstruction for simulation of compressible two-phase flows, *Int. J. Multiphase Flow.* 104 (July) (2018) 20–31.
12. **Sadin D. V., Golikov I. O., Davidchuk V. A.**, Simulation of a shock wave interaction with a bounded inhomogeneous gas-particle layer using the hybrid large-particle method, *Numerical Methods and Programming.* 22 (1) (2021) 1–13 (in Russian).
13. **Sadin D. V.**, A modified large-particle method for calculating unsteady gas flows in a porous medium, *Comput. Math. Math. Phys.* 36 (10) (1996) 1453–1458.
14. **Sadin D. V., Lyubarskii S. D., Gravchenko Y. A.**, Features of an underexpanded pulsed impact gas-dispersed jet with a high particle concentration, *Technical Physics.* 62 (1) (2017) 18–23.
15. **Sadin D. V.**, Simulation of the pulsed outflow of air and fine powder mixture, partially filling the discharge channel, *Scientific and Technical Journal of Information Technologies, Mechanics and Optics.* 22 (1) (2022) 187–192 (in Russian).

16. **Shirokova E. N.**, A numerical study of the expansion of a gas-particles mixture with axial symmetry, *Scientific and Technical Journal of Information Technologies, Mechanics and Optics*. 21 (4) (2021) 606–612 (in Russian).
17. **Nigmatulin R. I.**, Dynamics of multiphase media, In 2 Vols. Hemisphere Publ. Corp., New York, USA, 1990.
18. **Ivandaev A. I., Kutushev A. G., Rudakov D. A.**, Numerical investigation of throwing a powder layer by a compressed gas, *Combustion, Explosion and Shock Waves*. 31 (4) (1995) 459–465.
19. **Sadin D. V.**, TVD scheme for stiff problems of wave dynamics of heterogeneous media of nonhyperbolic nonconservative type, *Comput. Math. Math. Phys.* 56 (12) (2016) 2068–2078.
20. **Sadin D. V.**, A modification of the large-particle method to a scheme having the second order of accuracy in space and time for shockwave flows in a gas suspension, *Bulletin of the South Ural State University. Ser. Mathematical Modelling, Programming & Computer Software (Bulletin SUSU MMCS)*. 12 (2) (2019) 112–122 (in Russian).
21. **Quirk J. J., Karni S.**, On the dynamics of a shock-bubble interaction, *J. Fluid Mech.* 318 (10 July) (1996) 129–163.
22. **Wang M., Si T., Luo X.**, Experimental study on the interaction of planar shock wave with polygonal helium cylinders, *Shock Waves*. 25 (4) (2015) 347–355.

СПИСОК ЛИТЕРАТУРЫ

1. **Huilin L., Gidaspow D., Bouillard J., Wentie L.** Hydrodynamic simulation of gas-solid flow in a riser using kinetic theory of granular flow // *Chemical Engineering Journal*. 2003. Vol. 95, No. 1–3. Pp. 1–13.
2. **Zi C., Sun J., Yang Y., Huang Z., Liao Z., Wang J., Yang Y., Han G.** CFD simulation and hydrodynamics characterization of solids oscillation behavior in a circulating fluidized bed with sweeping bend return // *Chemical Engineering Journal*. 2017. Vol. 307. 1 January. Pp. 604–620.
3. **Gao X., Li T., Rogers W. A., Smith K., Gaston K., Wiggins G., Parks J. E.** Validation and application of a multiphase CFD model for hydrodynamics, temperature field and RTD simulation in a pilot-scale biomass pyrolysis vapor phase upgrading reactor // *Chemical Engineering Journal*. 2020. Vol. 388. 15 May. P. 124279.
4. **Luge I. A., Bentzon J. R., Klingaa C. G., Walther J. H., Anabaraonye B. U., Fosbuhl P. L.** Scale attachment and detachment: The role of hydrodynamics and surface morphology // *Chemical Engineering Journal*. 2022. Vol. 430. Part 2. 15 February. P. 132583.
5. **Волков К. Н., Емельянов В. Н.** Моделирование крупных вихрей в расчетах турбулентных течений. М.: Физматлит, 2008. 368 с.
6. **Гарбарук А. В.** Современные подходы к моделированию турбулентности. СПб.: Изд-во Политехнического ун-та, 233. 2016 с.
7. **Исаев С. А., Лысенко Д. А.** Тестирование численных методов, конвективных схем, алгоритмов аппроксимации потоков и сеточных структур на примере сверхзвукового течения в ступенчатом канале с помощью пакетов CFX и FLUENT // *Инженерно-физический журнал*. 2009. Т. 2 № .82. С. 326 – 330.
8. **Тишкин В. Ф., Гасилов В. А., Змитренко Н. В., Кучугов П. А., Ладонкина М. Е., Повешенко Ю. А.** Современные методы математического моделирования развития гидродинамических неустойчивостей и турбулентного перемешивания // *Математическое моделирование*. 2020. Т. 32. № 8. С. 57–90.
9. **Shi J., Zhang Y.-T., Shu C.-W.** Resolution of high order WENO schemes for complicated flow structures // *Journal of Computational Physics*. 2003. Vol. 186. No. 2. Pp. 690–696.
10. **Li J., Shu C.-W., Qiu J.** Multi-resolution HWENO schemes for hyperbolic conservation laws // *Journal of Computational Physics*. 2021. Vol. 446. 1 December. P. 110653.
11. **Wang B., Xiang G., Hu X. Y.** An incremental-stencil WENO reconstruction for simulation of compressible two-phase flows // *International Journal of Multiphase Flow*. 2018. Vol. 104. July. Pp. 20–31.
12. **Садин Д. В., Голиков И. О., Давидчук В. А.** Моделирование взаимодействия ударной волны с ограниченным неоднородным слоем газозвеси гибридным методом крупных частиц // *Вычислительные методы и программирование*. 2021. Т. 1 № .22. С. 1–13.



13. **Садин Д. В.** Модифицированный метод крупных частиц для расчета нестационарных течений газа в пористой среде // Журнал вычислительной математики и математической физики. 1996. Т. 10 № .36. С. 158–164.
14. **Садин Д. В., Любарский С. Д., Гравченко Ю. А.** Особенности недорасширенной импульсной импактной газодисперсной струи с высокой концентрацией частиц // Журнал технической физики. 2017. Т. 1 № .87. С. 22–26.
15. **Садин Д. В.** Моделирование импульсного истечения смеси воздуха и мелкодисперсного порошка, частично заполняющего выбросной канал // Научно-технический вестник информационных технологий, механики и оптики. 2022. Т. 1 № .22. С. 187–192.
16. **Широкова Е. Н.** Численное исследование разлета смеси газа и частиц с осевой симметрией // Научно-технический вестник информационных технологий, механики и оптики. 2021. Т. 4 № .21. С. 606–612.
17. **Нигматулин Р. И.** Динамика многофазных сред. Ч. 1. М.: Наука, 464 .1987 с.
18. **Ивандаев А. И., Кутушев А. Г., Рудаков Д. А.** Численное исследование метания слоя порошка сжатым газом // Физика горения и взрыва. 4 № .1995. С. 63–70.
19. **Садин Д. В.** TVD-схема для жестких задач волновой динамики гетерогенных сред негиперболического неконсервативного типа // Журнал вычислительной математики и математической физики. 2016. Т. 56. № 12. С. 2098–2109.
20. **Садин Д. В.** Модификация метода крупных частиц до схемы второго порядка точности по пространству и времени для ударно-волновых течений газозвеси // Вестник Южно-Уральского государственного университета. Сер. Математическое моделирование и программирование. 2019. Т. 12. № 2. С. 112–122.
21. **Quirk J. J., Karni S.** On the dynamics of a shock-bubble interaction // Journal of the Fluid Mechanics. 1996. Vol. 318. 10 July. Pp. 129–163.
22. **Wang M., Si T., Luo X.** Experimental study on the interaction of planar shock wave with polygonal helium cylinders // Shock Waves. 2015. Vol. 25. No. 4. Pp. 347–355.

THE AUTHOR

SHIROKOVA Elena N.

Military Space Academy named after A.F. Mozhaysky

13 Zhdanovskaya St., St. Petersburg, 197198, Russia

shirokhelen-78@mail.ru

ORCID: 0000-0002-8188-2003

СВЕДЕНИЯ ОБ АВТОРЕ

ШИРОКОВА Елена Николаевна — кандидат химических наук, преподаватель Военно-космической академии имени А. Ф. Можайского.

197198, Россия, Санкт-Петербург, Ждановская ул., 13

shirokhelen-78@mail.ru

ORCID: 0000-0002-8188-2003

Received 17.04.2022. Approved after reviewing 17.05.2022. Accepted 17.05.2022.

*Статья поступила в редакцию 17.04.2022. Одобрена после рецензирования 17.05.2022.
Принята 17.05.2022.*